INDIAN JOURNAL OF SCIENCE AND TECHNOLOGY

RESEARCH ARTICLE

Influence of Change in the Apparent Contact Area, Temperature and Vacuum on Tribo Response of Al6061 and EN8 Pair

M S Vinay[1,2]*, S Ranganatha[3], Madeva Nagaral[4]

1 Research Scholar, Mechanical Engineering Department, University Visvesvaraya College of Engineering, Bangalore University, Bangalore, India
2 Assistant Professor, Mechanical Engineering Department, School of Engineering, Dayananda Sagar University, Bangalore, India
3 Professor, Mechanical Engineering Department, University Visvesvaraya College of Engineering, Bangalore University, Bangalore, India
4 Deputy manager, Aircraft Research and Design Centre, HAL, Bangalore, India

OPEN ACCESS

Received: 07.06.2021
Accepted: 04.07.2021
Published: 24.08.2021

Citation: Vinay MS, Ranganatha S, Nagaral M (2021) Influence of Change in the Apparent Contact Area, Temperature and Vacuum on Tribo Response of Al6061 and EN8 Pair. Indian Journal of Science and Technology 14(28): 2368-2379. https://doi.org/10.17485/IJST/v14i28.1046

* **Corresponding author**.

vinnu.ms@gmail.com

Funding: None

Competing Interests: None

Published By Indian Society for Education and Environment (iSee)

ISSN
Print: 0974-6846
Electronic: 0974-5645

Abstract

Objective: Aluminium and its alloys components are used in aero and space industries where in many cases trioboloading prevails. In space application, in addition to triboloading, the components should also perform in the absence of atmosphere. In the present investigation, attempted has been made to simulate the field conditions in the laboratory by sliding Al6061 alloy pin of different diameters in a vacuum at different temperatures using a vertically configured pin-on-disc test rig. **Method:** The pin diameters were 2, 4, and 6mm and the testing temperatures were 373, 473, and 573K. The normal contact pressure was 0.625MPa and the sliding speed was 0.5ms-1 and both were constant throughout the experiment. The coefficient of friction was monitored using a PC and the worn pin surface was studied in scanning-electron-microscope. **Findings**: The result showed that the coefficient of friction at sliding temperatures 373 and 473K was found to be dependent on apparent contact area i.e., pin diameters 2, 4, and 6mm. The coefficient of friction was found to be 3.27 and 2.69 for pin diameter 2mm at temperature 373 and 473K whereas the coefficient of friction was of the range 1.36 to 0.33 for the pin of diameter 4 and 6mm. The scanning-electron-microscopic study revealed uniform plastic deformation for pin diameter of 2mm and non-uniform plastic deformation accompanied with abrasion extrusion phenomenon for the pin of diameters 4 and 6mm. The coefficient of friction at sliding temperature 573K was found to be insensitive to the apparent contact area. The coefficient of friction was in the range of 1.24 to 2.30. The SEM study revealed a large scale of non-uniform plastic deformation accompanied by abrasion, tearing of ridges, extrusion of both ridges, and entrapped wear debris. **Novelty**: It is a generic study for understanding the response of aluminium for tribo loading which.

Keywords: Pin on Disc (POD); Scanning Electron Microscope (SEM); High Temperature; Vacuum; Coefficient of Friction; Al6061 Aluminium Alloy 1

1 Introduction

Aluminium and its alloys are used in industries, aerospace, and space applications. The engineering components of aluminium and its alloys used in the above application are subjected to relative motions resulting in friction and wear of components. The friction is a passive force that results in bringing down the efficiency of operation of any equipment. The wear of component results in the replacement of worn-out components andextreme case calls for total replacement of equipment. The wear results in the loss of utility of equipment due to downtime and new capital investment due to the replacement of equipment. The ill effect of wear could be taken care of in usual applications but not feasible in the case of space application. In space applications, both temperature and environment contribute to influencing the response of the tribo system. Many attempts have been carried out by different researchers in understating the tribo response of the system in both vacuum and elevated temperature.

Wang et al.[(1)] for understanding hot extrusion of Aluminium, conducted experiments using a ball-on-disc test rig at elevated temperature using 7475 aluminium alloy and steel pair. The result showed that the coefficient of friction increased with an increase in test temperature and was attributed to large-scale plastic deformation and altered stress and strain state with temperature change. Vilaseca et al.[(2)] for understanding the; soldering,adhesion and wear of die casting tools in the aluminium die casting industry, conducted tests at elevated temperature using a ball-on-disc test rig. The experiments were conducted using die tool material uncoated and coated by the PVD method. The author concludes that the test results could be used for the proper design of a die-casting operation.Pujante et al.[(3)] using AA2017 balls and AISI H13 tool steel whose surface was engineered, conducted experiments at different temperatures up to 450°C in a linear reciprocating sliding test rigThe result showed that the test temperature influenced the wear mechanisms which were abrasive, the compacted layer of aluminium debris, and the aluminium transfer layer. The tool surface profile did not have much bearing on gross material transfer whereas the surface profile influenced the micro-wear mechanism.

Pellizzari[(4)] conducted experiments using a block-on-disc test rig for understanding tribo response of 6068 aluminium alloy and nitride, PVD duplex and CVD coated tool steel whose surface finish was engineered for simulating extrsion. The test result showed that engineered surface samples perform well due to higher load-bearing capacity and in particular duplex – PVD samples prevented a chemical attack of hot aluminium. The nitrated surface due to affinity of aluminium and iron was poorly performed. The coated surface revealed a stable friction coefficient and good surface finish because of build-up of the aluminium layer resulting in a better surface finish. Murakami et al.[(5)] conducted experiments using a pin-on-disc test rig at different temperatures. The aluminium pin made out of alloy 5052 was slid against different grades disc of tool steels. The discs were made out of Si_3N_4–8mass%Al_2O_3–6mass%Y_2O_3, AISI H13steel, AISI52100 steel, Inconel 600, ZrO_2–3mol%Y_2O_3, WC-6 mass% Co and BN-50 mass % Ni. The SEM and EDS analysis was carried out on a worn-out surface. The result showed that the tool material AISI H13, AISI 5200, and BN -50 mass % Nickle showed stable sliding with a Coefficient of friction of the order 0.4 – 0.5 and higher specific wear rates. The AISIH13steel, ZrO_2–3 mol%Y_2O_3, and WC-6mass% resulted in smaller wear loss. ZrO_2–3mol%Y_2O_3, WC-6 mass% CO disc exhibited unstable sliding with friction coefficient as high as 0.6. The SEM and EDS studies showed a large amount of aluminium and oxygen on worn-out die steel materials. A lesser amount of aluminium and oxygen were found on Inconel 600 WC-6 mass% CO and BN-50mass%Ni material. Oxygen pickup was observed on the worn-out surface of the aluminium. Kumar and Kumar[(6)] conducted experiments using a pin-on-disc test rig for characterizing tribo response of laser textured aluminium 6061 and 7071 alloys. The were dimples of circles, squares, and triangles. The textured surfaces improved the tribo response of aluminium alloy and the triangular texture resulted in the smallest Coefficient of friction of the order 0.170 – 0.184.

Gharam et al.[(7)] conducted experiments at elevated temperatures using a pin-on-disc test rig for evaluating tribo response of cast 319 grade aluminium and carbon-based coating pair. The test was conducted at an elevated temperature up to 400 °C. The coating of B_4C and hydrogenated diamond-like-carbon (DLC) was incorporated on the harder steel surface. The phenomenon of columnar grain boundary failure, aluminium transfer and absence of hydrogen and hydroxyl on carbon transfer layer influence the tribo response Bhowmick et al.[(8)] conducted experiments at elevated temperature using apin-on-disc test rig for evaluating tribo response of Si, O containing hydrogenated DLC coating and aluminium alloy casting. The study was conducted using aluminium and multilayer DLC coatings consisting of a top layer of H-DLC and the inner layer rich in Si and O as tribo pairs. The results showed that above 473 K testing temperature, the DLC coating exhibited higher Coefficient of friction and wear. The aluminium and a-C:H/a-Si:O coating pairs performed better up to 400 °C and also resulted in a low wear rate attributed to soft passivation of carbon and silicon coating and transfer layer and bulk graphitization of coating revealed in micro-Raman Spectro studies. The scanning-electron-microscope study revealed the formation of a transfer layer on the aluminium contact surface when tested against aluminium itself. The cross-sectional transmission electron microscopic study on the transfer layer formed at 400°C showed the presence of amorphous carbon with traces of SiC. The X-ray photoelectron spectroscopy study revealed the formation of C-OH, C-H, and Si-O bonds. Domitner et al.[(9)] used a strip drawing tribo system for characterizing the tribo response of tool steel and aluminium alloys. Experiments were conducted using aluminium alloy in

T4 and naturally aged conditions. Steel was used as a pin and aluminium was used as a strip sliding speed and normal loads were varied The result showed that the coefficient of friction increased with an increase in sliding distance. The average coefficient of friction was found to be in the range 0.09 – 0.17. The transfer of aluminium on the pin increases the Coefficient of friction. The work hardening of aluminium was found to influence the tribo response.

Selvam et al.[10] conducted experiments at elevated temperatures using a pin-on-disc (POD)test rig for characterizing the tribo response of flyash-aluminium 6061 compositesThe mechanism of wear in case of aluminium alloy was found to be adhesion and large scale plastic deformation and whereas in the case of composite, the mechanism was adhesion, plastic deformation, and oxidation. Ferreira et al.[11] conducted experiment at normal with elevated temperature using sphere- on –plate test rig for evaluating tribo response of functionally graded aluminium. The graded aluminium showed two distinct metallurgicallybonded layers called A and B. Layer A was consisting of Al-matrix reinforced by 53.4 vol% of hard quasi crystal α-$Al_{12}(Fe,Mn,Cr)_3Si$ which was homogeneously distributed. Layer B was consisting of hypo-eutectic Al-Si alloy. At room temperature, layer A resulted in a low Coefficient of friction of the order 0.2 and wear rate was less by one order of magnitude compared to that of layer B and attributed to protective and compacted aluminium rich oxide layer formed on layer A. Essa et al.[12] conducted experiments at different temperatures, normal load, and sliding speed using apin-on-disc test rig for evaluating tribo response of M50 steel reinforced with Al_2O_3 and/ or graphite nanoparticles. The samples studied were M50 alloy steel (M), M50 reinforced with 10wt% Al_2O_3 (MA), and M50 hybrid reinforced with Al_2O_3 and grapheme (MAG). The test sample surface was engineered by polishing using 0.05-micrometer diamond paste The counter body was silicon nitride balls. The result showed that MAG exhibited better tribo response compared to M and MA and which was attributed to the synergic effect of Al_2O_3 and graphene.

Zhu et al.[13] conducted experiments at elevated temperatures for evaluating tribo response of aluminium and ZrO_2-C composite using a pin-on-disc test rig. The results of the test at elevated temperatures showed that all the composites will have similar trends in wear loss with respect to change in velocity and load. The wear loss at 373 K was found to increase with speed and found to be maximum at an approximate speed of 0.6 m/s followed by a decrease with an increase in velocity. Whereas at a testing temperature of 473 K the mass loss increased with an increase in sliding speed. The increase in a molar ratio of C/ ZrO_2 always improved the tribo response. The wear mechanisms identified were adhesive and plastic deformation. Gecu et al.[14] studied the tribo response of 304 stainless steel reinforced AA7075 aluminium composite using a ball-on-disc test rigAA7075 alloy and 304 SS reinforced 7075 aluminium alloy with and without MAO were studied. The bimetal composite results in improved wear performance and was attributed to the phases θ-Fe_4Al_{13}, η-Fe_3Al_5, and Al_2O_3 Zhu et al.[15] conducted experiments at elevated temperatures using a pin-on-disc test rig for characterizing tribo response of aluminium matrix composites reinforced with $Al_3Zr + \alpha$-Al_2O_3. The study was conducted in situ. The pin was made of composite and the disc was hardened steel. The result showed that temperature, speed, and load influenced the tribo response. The wear rate at 373 K was found to depend on sliding speed and found that the wear rate increased to a maximum value and decreased with a further increase in sliding speed. The wear rate was found to monotonically decrease with an increase in sliding speed at test temperature 473 K. At test temperature 473 K and sliding speed of 0.6 m/s, the sliding was found to be transiting from stable to unstable at an approximate load of 50 N. The wear loss was found to improve with increasing reinforcement but the Al_3Zr phase was found to be detrimental. Increased load and test temperature resulted in abrasive, oxidation, and adhesive wear modes.

Bajwa[16] evaluated the tribological response lubricated with water of nickel based composite coatings. The evaluation find importance in designing of marine vessels, conventional power plants, tidal and wave energy equipments and other water lubricated industrial machinery. Experiment were conducted using a modified Ball-On-Disc assembly where facility for water lubrication was provided. The nickel coatings with nano particle like Al_2O_3, SiC and ZrO_2 was incorporated using electro deposition process. The author optimized the process parameters for a good performing coating in tribo-system. The result showed that the tribo performance of composite coating was found to be superior with 30 % decrease in specific wear rate and twice improvement in corrosion specific wear rate and twice improvement in corrosion resistance of nano particle composite nickel coating when compared to conventional nickel coating. The covalent bonding between tribo system and lubricant is also one of the factor in improving tribo response. Poirier et al.[17] conducted experiments using POD cyclic corrosion and custom based heating system for characterizing stainless coating on aluminium substrate. Arc spraying and cold spraying technique were used for coating stainless steel. The results of POD test showed that the wear performance of stainless steel coated on aluminium were comparable with the wear performance of gray cast iron. The cold sprayed coating performed better in case of corrosion resistance and thermal cycling resistance when compared to spray coatings. The author also evaluated a cold sprayed bond coat and hot sprayed top coat called duplex coating and found superior to both arc spray coating and cold spray coating. Yadav and Dixit[18] used slurry disintegration analyzer for erosion test and POD for wear test in characterizing aluminium silicon alloy and its two composite reinforce with SiC and $TiBr_2$. Field emission scanning electron microscope and energy dispersive microscope analysis showed that the erosion was insatiated at Al-Si interface. The erosion test conducted in aqueous

medium results showed that the material removal rate was dependent on target material. The results of high stress abrasive test showed that the reinforced particles i.e., SiC and $TiBr_2$ improved the abrasive performance when compared to Al-Si based alloy. Features like fracture, micro cutting, cracks, ploughing and crater formation phenomenon were observed as wear mechanism.

Shinde et al.[19] reviewed the tribological response of nano particulated aluminium metal composite. The authors concluded that the wear and friction being system dependent phenomenon were found to be influenced by parameters like reinforcement, method of processing composite, different phases in microstructure, stress level, relative speeds, contact condition and system generated in situ tribolayer. Kumar et al.[20] Chartersied physical, mechanical and tribological response of Al 6061 composite with particulated nano sized ZrO_2. The wear results showed that addition of nano sized ZrO_2 particles improved wear response. Shafqat et al.[21] studied mechanical, electrochemical and tribo response of Al 6061 composite particulated with nano sized particles of boron carbide and graphene. The wear results showed that the presence of nano sized particles in the composite improved both wear and coefficient of friction. Chandla et al.[22] reviewed the research work carried out to understand mechanical and tribological behavior of stirr cast Al 6061composite. The results of the researchers revealed that there is substantial improvement both mechanical and tribological response of composite Al 6061 alloy

The literature shows the research work of different author aimed in evaluating tribo response of a system where parameters like normal load, sliding speed, different coating material, testing temperature and vacuum were considered. In the present investigation the author aimed at understanding the influence of apparent contact area on tribo response of a system in which temperature was varied in a vacuum environment. The study is of a generic in nature and finds utility in tackling tribo problem encountered in elevated temperature and vacuum environment.

2 Experimental Details

A set of experiments using cylindrical Al-6061 aluminium alloy pin of different diameters were conducted by sliding against a hardened EN-8 steel disc. The Al-6061 aluminium alloy material pin was machined to a cylindrical pin of diameters of 2 mm, 4 mm, and 6 mm respectively. Figure 1 shows the schematic representation of cylindrical pins used in research work.

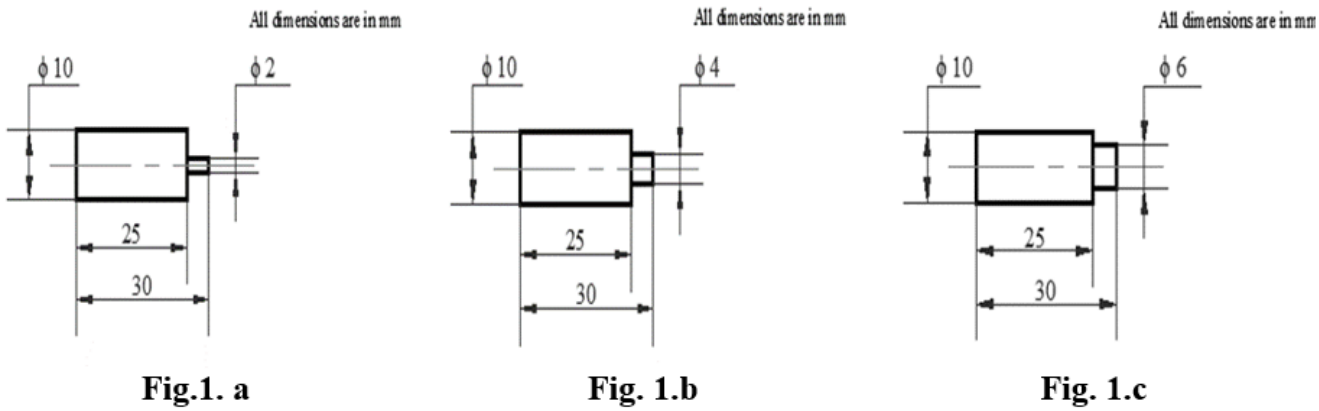

Fig 1. The drawing with dimensions of all cylindrical pins

All the pins of different diameters were machined out of a cast Al-6061 aluminium alloy. Figure 1a shows the drawing of a pin of 2 mm diameter. Figure 1b shows the drawing of a pin of 4 mm diameter. Figure 1c shows the drawing of a pin of 6 mm diameter.

The specially configured pin-on-disc test rig was used to conduct experiment. The testrig houses vertical configured Pin-On-Disc in a chamber where both temperature and vacuum are monitered.

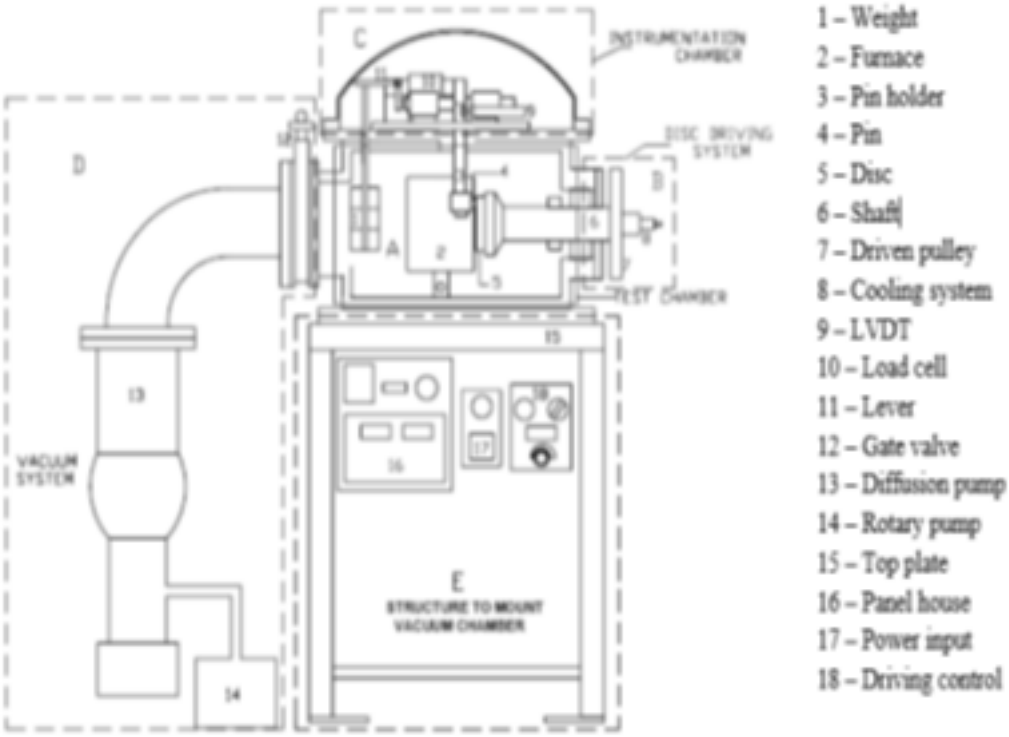

Fig 2. Schematic view of specially configured pin-on-disc [23]

The specially fabricated test rig has subsystems A, B, C, D, and E. Subsystem A is a chamber in which the test pin, disc, heating furnace, and provision for normal load applications are provided. Subsystem B accommodates the disc driving system. Subsystem C is a chamber in which instrumentation is housed.

The aluminium pin was made to establish contact against the hardened EN-8 steel disc. The normal load was applied in the leverage system wherein the load was magnified by approximately 1.5 times.

Experiments were conducted at temperatures 373 K, 473 K, and 573 K respectively. The pin diameters used in the experiment were 2 mm, 4 mm and 6 mm respectively. The normal contact pressure was 0.625 MPa. The sliding speed was 0.5 ms^{-1}. All the experiments were conducted in a vacuum with a vacuum level of 4×10^{-4} Pa. The frictional force was monitored using a personal computer. The worn-out surface of the pin was studied in SEM for understanding wear mechanism and to correlate observed dependency of coefficient of friction with experimental variables like testing temperature, apparent contact area, and vacuum.

3 Results and Discussion

Experiments were conducted in vacuum using Al 6061 aluminium alloy pins of diameters 2 mm, 4 mm, and 6 mm, which were slid against hardened EN-8 steel disc at three different temperatures which were 373 K, 473 K, and 573 K. The sliding speed was $0.5ms^{-1}$ and the normal contact pressure was 0.625 MPa. The present research work was aimed at understanding the parametric effect of variation in apparent contact area maintaining constant intensity of pressure on tribo response of contacting pairs. For obtaining constant stress intensity of 0.625 MPa using available discrete weights in the laboratory, the diameters of 2 mm, 4 mm and 6 mm of pins were chosen.

3.1 Sliding Temperature – 373 K

The typical dependency of coefficient of friction at test temperature with sliding time is shown in Figure 3.

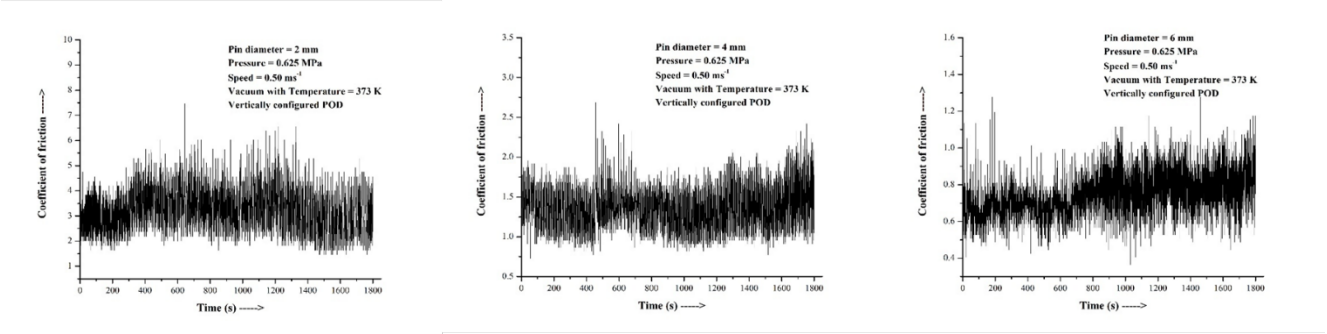

Fig 3. a) Dependency of coefficient of friction on sliding time, **b)** Dependency of coefficient of friction on sliding time, **c)** Dependency of coefficient of friction on sliding time

Figure 3a shows the dependency of coefficient of friction with a sliding time for study of pin of diameter 2 mm in vacuum at temperature 373 K. The sliding was found to be stable and the average coefficient of friction was found to be 3.27.

Figure 3b shows the dependency of coefficient of friction with a sliding time for an experiment conducted at test temperature 373 K in a vacuum for a pin of 4 mm diameter. The sliding was found to be stable with an average coefficient of friction was found to be 1.36.

Figure 3c shows the dependency of coefficient of friction with a sliding time at temperature 373 K in vacuum when 6 mm diameter was slid. The sliding was found to be stable and estimated average coefficient was 0.75.

3.2 Sliding Temperature – 473 K

The typical dependency of coefficient of friction at test temperature with sliding time is shown in Figure 4.

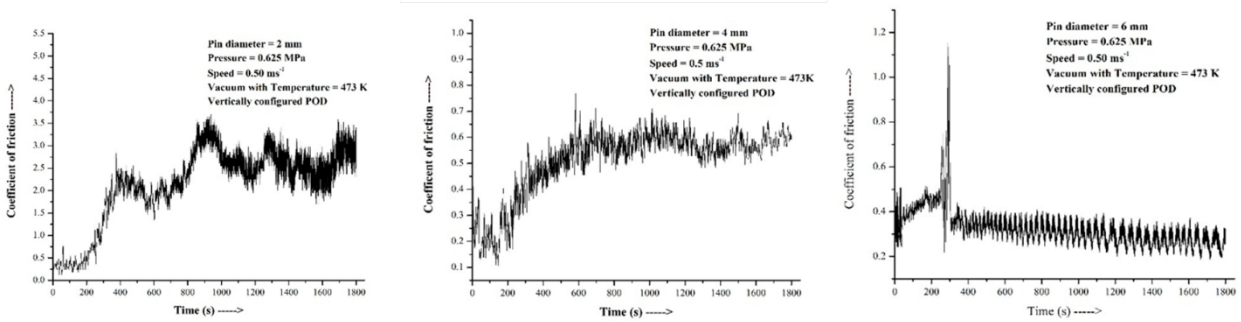

Fig 4. a) Dependency of coefficient of friction on sliding time, **b)** Dependency of coefficient of friction on sliding time, **c)** Dependency of coefficient of friction on sliding time

Figure 4a shows the dependency of coefficient of friction with a sliding time for an experiment conducted at test temperature 473 K in a vacuum for a pin of 2 mm diameter. The Coefficient of friction was found to be of the order of 0.45 over a sliding time of 0 to 200 s. The Coefficient of friction was found to gradually increase from 0.45 to an approximate value of 2.02 over a sliding time interval of 200 s to 800 s. The sliding was found to be steady from 800 s to the end of the experiment i.e., 1800 s. The average Coefficient of friction during this steady state of sliding was found to be 2.69

Figure 4b shows the dependency of co-efficient of friction with a sliding time for an experiment conducted at test temperature 473 K in vacuum for a pin of 4 mm diameter. The Coefficient of friction was found to gradually increase from 0 to approximately to a value of 0.37 over a sliding interval of time 0 to 600 s. The sliding was found to be steady over a time interval of 600 s and the end of the experiment i.e., 1800 s. The average Coefficient of friction was found to be 0.58 during the steady-state of sliding

Figure 4c shows the dependency of coefficient of friction with a sliding time for an experiment conducted at test temperature 473 K in vacuum for a pin of 6 mm diameter. The sliding was found to be steady throughout the sliding experiment except during an initial interval of time 0 to 300 s. The sliding during this initial interval was also considerably steady with an average coefficient of friction being slightly larger than the average coefficient of friction found during the steady-state of sliding which was over

the time interval of 300 s to the end of the experiment i.e., 1800 s. The average coefficient of friction during the steady-state of sliding was found to be 0.33.

3.3 Sliding Temperature – 573 K

The typical dependencies of coefficient of friction at test temperature with sliding time are shown in Figure 5.

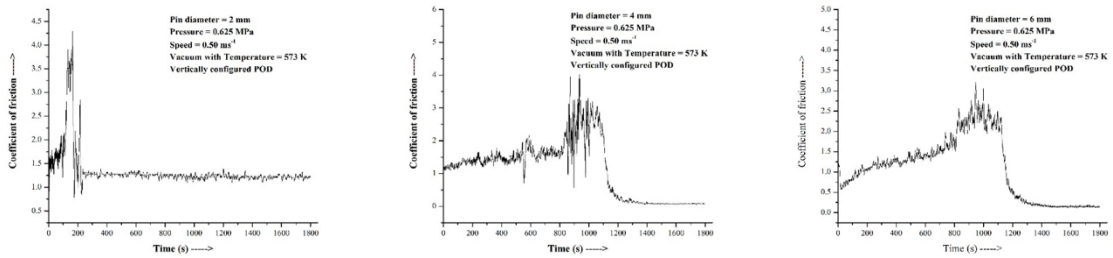

Fig 5. a) Dependency of coefficient of friction on sliding time, **b)** Dependency of coefficient of friction on sliding time, **c)** Dependency of coefficient of friction on sliding time

Figure 5a shows the dependency of coefficient of friction with a sliding time for an experiment conducted at test temperature 573 K in vacuum for a pin of 2 mm diameter. The sliding was found to be unsteady during a sliding time interval of 0 to 150 s. The Coefficient of friction was found to increase during this unsteady sliding interval. The sliding was found to be steady during the time interval of 150 s to the end of the experiment. The average Coefficient of friction during the steady-state of sliding was found to be of the order 1.24.

Figure 5b shows the dependency of coefficient of friction with a sliding time for an experiment conducted at test temperature 573 K in vacuum for a pin of 4 mm diameter. The sliding was found to be steady expect a small interval of time of 825 to 1100 s. The average Coefficient of friction during the steady-state of sliding was found to be of the order 1.72.

Figure 5c shows the dependency of coefficient of friction with a sliding time for an experiment conducted at test temperature 573 K in vacuum for a pin of 6 mm diameter. The sliding was found to be non-steady during the time interval 0 to 800 s. The coefficient of friction during this non-steady-state of sliding was found to increase approximately from 0.5 to a value of 2. The sliding was found to be steady during a time interval of 800 s to 1200 s. The average coefficient of friction during the steady-state of sliding was found to be 2.30.

The average coefficient of friction during steady-state of sliding for pins of diameter 2 mm, 4 mm, and 6 mm slid in vacuum at temperature 373 K, 473 K, and 573 K are estimated from Figures 3, 4 and 5

The estimated average coefficient of friction and its dependency on sliding pin diameters and various sliding temperatures are tabulated in table 1 and is shown in bar chart Figure 6

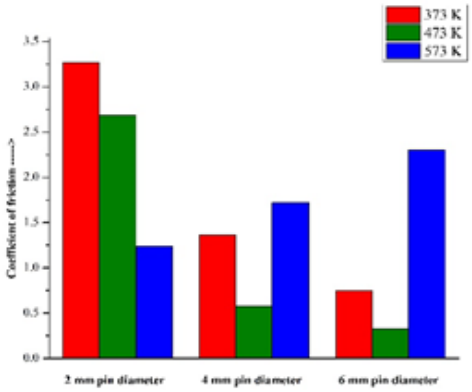

Fig 6. Co-efficient of friction at different temperature in the vacuum of pins of different diameter

The bar chart shows that irrespective of test temperature, the coefficient of friction for a pin of diameter 2mm is comparable. The coefficient of friction for 4mm and 6mm pin diameters at 373 K and 473 K are comparable range. The coefficient of friction at a sliding temperature of 573 K was in the comparable range for all the pin diameters i.e., 2mm, 4mm, and 6 mm. The effect of temperature at 373 K on sliding was not found whereas the changed apparent contact area influenced the coefficient of friction. The results of coefficient of friction at sliding temperature 473 K and 573 K showed that the effect of testing temperature was dominant when compared to effect of change in apparent contact area. At testing 473 K and 573 K the aluminium becoming more ductile resulted in increase in coefficient of friction.

3.4 Scanning Electronic Microscope Study

The pin surface for understanding the mechanism involved in sliding pins of different diameters at different sliding temperatures was studied in an SEM.

Figure 7 shows the scanning electron micrograph of a 2 mm diameter aluminium pin at 373 K slid at a speed of 0.5 ms^{-1} with the normal pressure of 0.625 MPa.

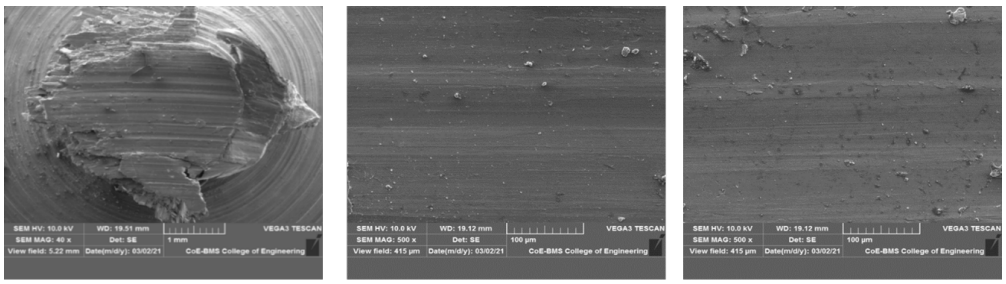

Fig 7. Scanning electron micrograph for the test at 373 K of pin diameter 2 mm

The micrograph in Figure 7a shows the full view of the pin tip at magnification 50X. The feature reveals gross abrasion and a small extent of extrusion which resulted in the formation of tile material at the trailing end.

The micrographs in Figure 7b and Figure 7c are the views at two different locations of pin surface with a magnification of 500X. The feature in both the micrograph reveals smooth morphology and large extent of uniform plastic deformation. which explains the observered dependency of coefficient of friction on sliding time.

Figure 8 shows the SEM of a 2 mm diameter aluminium pin at 473 K slid at a speed of 0.5 $ms^{-1}$with the normal pressure of 0.625 MPa.

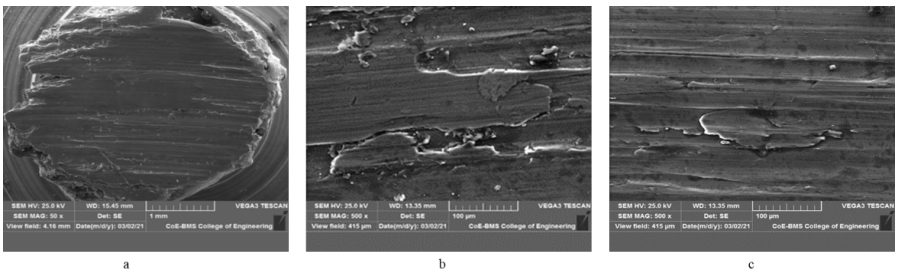

Fig 8. Scanning electron micrograph for the test at 473 K of pin diameter 2 mm

The micrograph in Figure 8a shows the full view of the pin tip at magnification 50X. The feature reveals abrasive sliding and extrusion effect which resulted in tail material at the trailing edge of the pin.

The micrographs in Figure 8b and in Figure 8c are the views at two different locations with a magnification of 500X. The feature in both micrographs shows a large extent of abrasion and extrusion. In particular, micrograph in Fig 8.b reveals breakage and extrusion of the ridge of the grooves. Both the micrograph reveals the feature of non-uniform plastic deformation.

Figure 9 shows the scanning electron micrograph of 4 mm diameteraluminium pin at 373 K slid at a speed of 0.5 ms^{-1} with the normal pressure of 0.625 MPa.

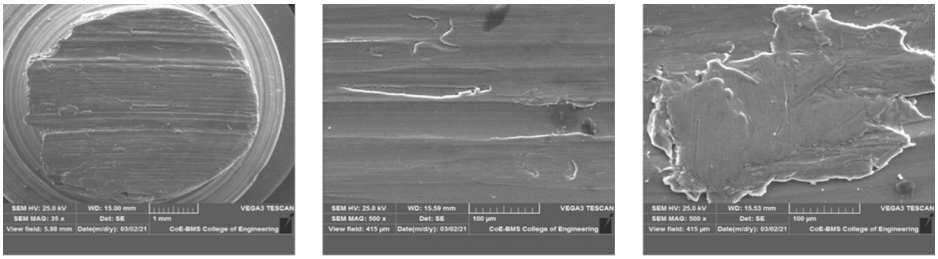

Fig 9. Scanning electron micrograph for the test at 373 K of pin diameter 4 mm

The micrograph Figure 9a shows the full view of the pin tip at magnification 50X. The features in the micrograph reveal macro abrasion and less extent of macro extrusion.The micrographs in Figure 9b and in Figure 9c are the views at two different locations with a magnification of 500X. The feature in micrograph in Figure 9b shows abrasion. The feature in micrograph Figure 9c shows the feature of extrusion of entrapped wear debris. Feature in both micrographs of Figure 9b and Figure 9c reveal non-uniform plastic deformation.

Figure 10 shows the scanning electron micrograph of 4 mm diameter aluminium pin at 473 K slid at a speed of 0.5 ms^{-1} with the normal pressure of 0.625 MPa.

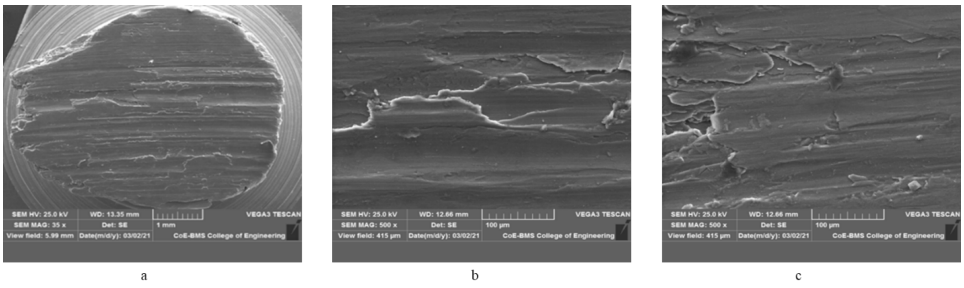

Fig 10. Scanning electron micrograph for the test at 473 K of pin diameter 4 mm

The micrograph Figure 10a shows the full view of the pin tip at magnification 35X. The feature in the micrograph reveals macro abrasion and a small extent of extrusion. The micrographs in Figure 10b and in Figure 10c are the views at two different locations with a magnification of 500X. Both the micrograph reveal a large extent of plastic deformation and extrusion of groove ridges. The morphology reveals non-uniform plastic deformation.

Figure 11 shows the scanning electron micrograph of a 6 mm diameter aluminium pin at 373 K slid at a speed of 0.5 ms^{-1} with the normal pressure of 0.625 MPa.

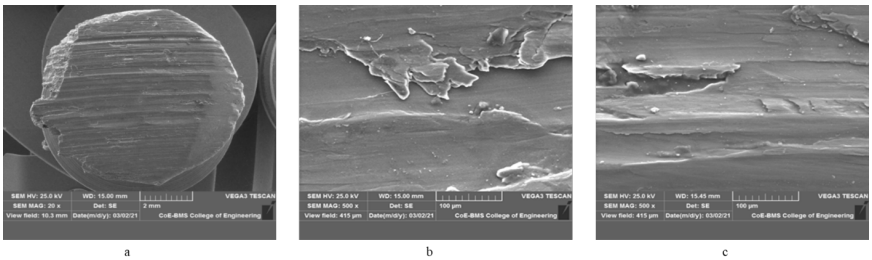

Fig 11. Scanning electron micrograph for the test at 373 K of pin diameter 6 mm

Figure 11a shows the full view of the pin tip at magnification 20X. The feature in the micrograph reveals gross abrasion. The micrographs in Figure 11b and in Figure 11c are the views at two different locations with a magnification of 500X. Both the micrograph reveals features of abrasion and extrusion of ridge material. The micrograph Figure 11b reveal the tearing features of ridge materials. The feature in both micrographs reveals non-uniform plastic deformation.

Figure 12 shows the scanning electron micrograph of 6 mm diameter aluminium pin at 473 K slid at a speed of 0.5 ms^{-1} with the normal pressure of 0.625 MPa.

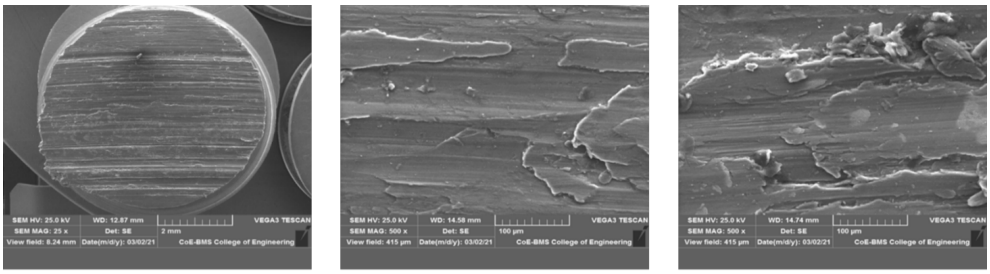

Fig 12. Scanning electron micrograph for the test at 473 K of pin diameter 6 mm

The micrograph Figure 12a shows the full view of the pin tip at magnification 25X. The feature in the micrograph revealsgross abrasion.

The micrographs in Figure 12b and in Figure 12c are the views at two different locations with a magnification of 500X. Both the micrographs reveal the feature of large-scale plastic deformation and extrusion. Micrograph Fig. 12.b shows the extrusion of grove material. The micrograph in Fig. c shows both extrusions of ridge material and entrapped wear debris.

Figure 13 shows full view micrographs of pin of diameter 2 mm, 4 mm and 6 mm at test temperature 573 K

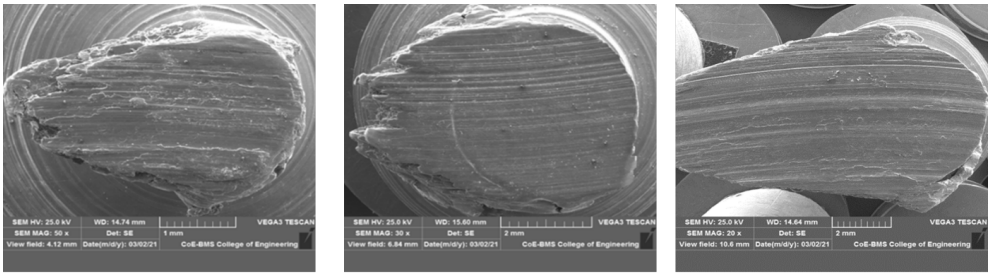

Fig 13. Scanning electron micrograph for the test at 573 K of pin diameter 2 mm, 4 mm, and 6 mm.

All the micrographs show macro abrasion and varied extent of macro extrusion which were reflected in the formation of tail material at the trailing edge of the pin. The extent of the tail material was found to be larger in the case of the pin with a diameter of 2 and 6 mm when compared to the pin of 4 mm diameter. The abrasion feature in the case of micrographs of Figure 13b and Figure 13c are comparable and different from the feature of micrograph Figure 13a. The abrasion feature in the micrograph Figure 13a shows the tearing of groove ridges.

Figure 14 shows full view micrographs of pin of diameter 2 mm, 4 mm and 6 mm at test temperature 573 K

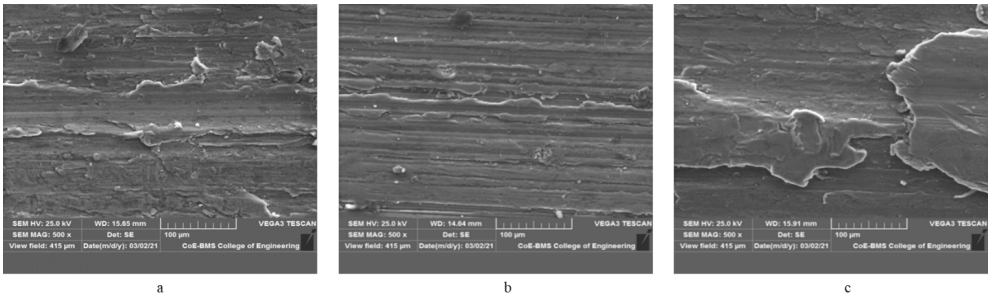

Fig 14. Scanning electron micrograph for the test at 573 K of pin diameter 2 mm, 4 mm, and 6 mm

Micrograph in Figure 14a shows the feature of abrasion, tearing of ridges, and less degree of extrusion. Micrograph in Figure 14b shows features of abrasion and extrusion of ridges without significant tearing of ridges. Micrograph in Figure 14c shows a large extent of plastic deformation and extrusion of both aluminium and entrapped wear debris. The features in all micrographs Figure 14a, Figure 14b and Figure 14c reveal non-uniform plastic deformation.

3.5 Summary – Micrography Study

The micrographs studied at test temperatures at 373 and 473 K reveal the following features:

1. The deformation feature for pin 2 mm at 373 and 473 K is more of uniform plastic deformation.
2. The deformation features of pins 4 and 6 mm at 373 and 473 K were found to be non-uniform plastic deformation accompanied by abrasive and extrusion mechanisms.
3. The deformation mechanism at 573 K for all the pin diameters was influenced by testing temperature and features of the micrograph revealed a large extent of plastic deformation, abrasion, and extrusion.
4. The observed dependency of the average coefficient of friction on the contact area which was guided by pin diameter was attributed to varied plastic deformation and wear phenomenon.

4 Conclusions

- The average coefficient of friction at temperatures 373 and 473 K was found to depend on the contact area i.e., pin diameters.
- The average coefficient of friction at 573 K was found to be not much influenced by contact area i.e., pin diameter of 2 mm, 4 mm, and 6 diameters.
- The coefficient of friction was found to be larger for lesser contact area (pin of 2mm diameter) when compared to larger contact area (pin of 4 and 6 mm diameter)
- The larger extent of uniform plastic deformation and the absence of micro-wear mechanisms like abrasion and extrusion were attributed to the observed larger magnitude of the average coefficient of friction in the case of a pin of 2 mm diameter.
- The lack of uniform deformation and existence of non-uniform plastic deformation accompanied by abrasion and extrusion, were attributed to the observed lesser average magnitude of the coefficient of friction in the case of pins of diameters 4 and 6 mm.
- The deformation mechanism at 573 K for pin diameters of 2 mm, 4 mm, and 6 mm are comparable. This is in consistent with the observed magnitude of co-efficient of friction for 2 mm, 4 mm, and 6 mm.
- The micrograph features for all pin diameters i.e., 2 mm, 4 mm, and 6 mm at 573 K revealed non-uniform plastic deformation accompanied by abrasive and extrusion phenomenon.

Limitations

- The present research is a generic in nature and attempt to be made for specific problems encountered in actual working machinery.

Scope for future studies

- Research study to be aimed in understanding the role of apparent contact area on tribo response with different combination of mating pairs where parameters like hardness difference, metallurgical compatibility, surface asperity and their size and distribution are considered.
- Research study to be aimed in understanding the role of different pressures level on tribo response while keeping different apparent contact areas.
- Numerical simulations to be considered.
- Subsurface studies of soft contacting surface to be considered.
- The elemental analysis of transfer layer and wear scar to be carried out.

References

1) Wang L, He Y, Zhou J, Duszczyk J. Effect of temperature on the frictional behaviour of an aluminium alloy sliding against steel during ball-on-disc tests. *Tribology International*. 2010;43:299–306. Available from: https://doi.org/10.1016/j.triboint.2009.06.009.

2) Vilaseca M, Molas S, Casellas D. High temperature tribological behaviour of tool steels during slidingagainst aluminium. *Wear*. 2011;272:105–109. Available from: https://doi.org/10.1016/j.wear.2011.07.007.
3) Pujante J, Pelcastre L, Vilaseca M, Casellas D, Prakash B. Investigations into wear and galling mechanism of aluminium alloy-tool steel tribopair at different temperatures. *Wear*. 2013;308:193–198. Available from: http://dx.doi.org/10.1016/j.wear.2013.06.015.
4) Pellizzari M. High temperature wear and friction behaviour of nitrided, PVD-duplex and CVDcoated tool steel against 6082 Al alloy. *Wear*. 2011;271:2089–2099. Available from: https://doi.org/10.1016/j.wear.2011.01.067.
5) Murakami T, Kajino S, Nakano S. High-temperature friction and wear properties of various sliding materials against aluminum alloy 5052. *Tribology International*. 2013;60:45–52. Available from: http://dx.doi.org/10.1016/j.triboint.2012.10.015.
6) Kumar PK, Kumar AS. Investigation of frictional characteristics of laser textured aluminium6061 and aluminium 7071 alloys under dry sliding conformal contactin pin on disc tribometer. *Materials Today Proceedings*. 2020. Available from: https://doi.org/10.1016/j.matpr.2020.02.735.
7) Gharam AA, Lukitsch MJ, Balogh MP, Alpas AT. High temperature tribological behaviour of carbon based (B4C and DLC) coatings insliding contact with aluminum. *Thin Solid Films*. 2010;519:1611–1617. Available from: https://doi.org/10.1016/j.tsf.2010.07.074.
8) Bhowmick S, Banerji A, Lukitsch MJ, Alpas AT. The high temperature tribological behavior of Si, O containing hydrogenated diamond-like carbon (a-C:H/a-Si:O) coating against an aluminum alloy. *Wear*. 2015;330-331:261–271. Available from: http://dx.doi.org/10.1016/j.wear.2015.01.072.
9) Domitner J, Silvayeh Z, Sabet AS, Oksuz KI, Pelcastre L, Hardell J. Characterization of wear and friction between tool steel and aluminum alloys in sheet forming at room temperature. *Journal of Manufacturing Processes*. 2021;64:774–784. Available from: https://doi.org/10.1016/j.jmapro.2021.02.007.
10) Selvam JDR, Dinaharan I, Mashinini PM. High temperature sliding wear behavior of AA6061/fly ash aluminum matrix composites prepared using compocasting process. *Tribology - Materials, Surfaces & Interfaces*. 2007;11:39–46. Available from: http://dx.doi.org/10.1080/17515831.2017.1299324.
11) Ferreira T, Koga GY, Oliveira ILD, Shyintikiminami C, Botta WJ, Bolfarini C. Functionally graded aluminum reinforced with quasicrystal approximant phases - Improving the wear resistance at high temperatures. *Wear*. 2020;15:462–463. Available from: https://doi.org/10.1016/j.wear.2020.203507.
12) Essa FA, Elsheikh AH, Yu J, Elkady OA, Saleh B. Studies on the effect of applied load, sliding speedand temperature on the wear behavior of M50 steelreinforced with Al2O3 and / or grapheme nanoparticles. *Journal of materials research andtechnology*. 2021;12:283–303. Available from: https://doi.org/10.1016/j.jmrt.2021.02.082.
13) Zhu H, Min J, Ai Y, Chu D, Wang H, Wang H. The reaction mechanism and mechanical properties of the composites fabricated in an Al-ZrO2-C system. *Materials Science and Engineering A*. 2010;527:6178–6183. Available from: https://doi.org/10.1016/j.msea.2010.07.001.
14) Gecua R, Yurekturkb Y, Tekoglub E, Muhaffelb F, Karaaslan A. Improving wear resistance of 304 stainless steel reinforced AA7075aluminummatrix composite by micro-arc oxidation. *Surface & Coatings Technology*. 2019;368:15–24. Available from: https://doi.org/10.1016/j.surfcoat.2019.04.029.
15) Zhu H, Jar C, Jinzhusong J, Zhao J, Zonghanxie. High temperaturedryslidingfrictionandwearbehaviorofaluminummatrixcomposites (Al3Zrþa-Al2O3)/Al. *Tribology International*. 2012;48:78–86. Available from: https://doi.org/10.1016/j.triboint.2011.11.011.
16) Bajwa RS. Electroplated Composite Coatings with Incorporated Nano Particles for Tribological Systems with the Focus on Water Lubrication. A thesis submitted in partial fulfilment of the requirements of Bournemouth University for the degree of Doctor of Philosophy. NanoCorr, Energy & Modelling Research Group Faculty of Science and Technology. 2016. Available from: http://eprints.bournemouth.ac.uk/24757/.
17) Poirier D, Legoux JG, Irissou E, Gallant D, Jiang J. Tim Potter and James Boileau Performance Assessment of Protective Thermal Spray Coatings for Lightweight Al Brake Rotor Disks. *J Therm Spray Tech*. 2019;28:291–304. Available from: https://doi.org/10.1007/s11666-018-0805-0.
18) Yadav PK, Dixit G. Investigation of High Stress Abrasive and Erosive Wear Behaviour of AA336/TiB2/SiC Ex Situ Composites . *Journal of Bio- and Tribo-Corrosion*. 2019;5:74. Available from: https://doi.org/10.1007/s40735-019-0256-2.
19) Shinde DM, Sahoo P, Davim JP. Tribological characterization of particulate-reinforced aluminum metal matrix nanocomposites: A review. *Advanced Composites Letters* . 2020;p. 1–28. Available from: https://doi.org/10.1177/2633366X20921403.
20) Kumar HSV, Kempaiah UN, Nagaral M, Revanna K. Investigations on Mechanical Behaviour of Micro B4C Particles Reinforced Al6061 Alloy Metal Composites. *Indian Journal Of Science And Technology* ;14:1855–1863. Available from: https://doi.org/10.17485/IJST/v14i22.736.
21) Shafqat QA, Rafi-Ud-Din M, Shahzad M, Khan S, Mehmood, Waqar A, et al. Mechanical, tribological, and electrochemical behavior of hybrid aluminum matrix composite containing boron carbide (B4C) and graphene nanoplatelets. *Journal of Materias*. 2019;34(18). Available from: https://10.1557/jmr.2019.242.
22) Chandla NK, Kant S, Goud MM. Mechanical, tribological and microstructural characterization of stir cast Al-6061 metal/matrix composites - a comprehensive review . *Sādhanā* . 2021;46:47. Available from: https://doi.org/10.1007/s12046-021-01567-7.
23) Ranganatha S, Layer T. 2008. Available from: https://etd.iisc.ac.in/handle/2005/871.